OVERHEAD LINES GALLOPING AND TURBULENT WIND

O. CHABART and J.L. LILIEN
Transport et Distribution de l'Energie Electrique
Institut d'Electricité Montefiore,
Sart Tilman, Liège

Introduction

Galloping is a low frequency, large amplitude, wind-induced vibration of both single and bundle conductors of overhead lines, with a single or a few loops of standing waves per span. The ice accretion on the conductor has the effect of modifying the cross-sectional shape of the conductor, so that it becomes aerodynamically unstable. Due to the large amplitudes occurring during this phenomena, electrical and mechanical damages may lead to very important financial costs for the utilities. Galloping is studied for more than 70 years, but the definitive solution to avoid this problem has not yet been found. The analytical approach to reproduce some real cases is quite difficult because there are a lot of uncertainty on the data. For instance, the ice shape and its distribution on all the span, the space time distribution of the turbulent wind, the torsional stiffness of the system and so for but with some realistic assumptions it is possible to obtain some results not too far from the real observations.

Since 1987, this problem is studied in the TDEE department (Transmission and Distribution of Electrical Energy) in collaboration with Laborelec (Belgium) and some international electrical utilities (KANSAI EPCO (Japan) f.e.). We are also involved in the galloping task force of the CIGRE. And since 1994, the galloping is a part of a ARC project (subsidied by the «Communauté Française de Belgique») dealing with the vibration problems of cable structures (in collaboration with the Mechanical Department and the Civil Department of University of Liege). The department is also the designer of a new kind of countermeasure device (so called 'TDD') produced by Dulmison U.K. Two programs have been developed. One is based on the simplified equations of the problem. It is mainly used to search the fundamental parameters involved in the mechanisms. The other one resolves the complete space-time equations, but is obviously more expensive in CPU time.

This paper deals with the specific problem of wind model wich has to be used for galloping studies. Generaly, constant (in space and time) wind is considered. In this paper another model is used.

Turbulence description

The turbulence in the atmospheric layer near the ground is the subject of many papers [1,2]. This factor is also very important for the design of large constructions like bridges and tall buildings [3]. In the field of overhead transmission lines, it is more often taken into account in the problem of aeolian vibrations [8]. But for galloping it is not the topic of many studies. The analytical simulation has been chosen to outline the effect of turbulence on galloping. In fact it can be divided into two different parts, the first is the wind speed variation which has a direct influence on the aerodynamical load of the line. This is mainly important for the large scale of turbulence. The second is due to the modification of the flow around the cable for the smaller scale of turbulence. And this effect may considerably modify the aerodynamic coefficients of bluff bodies which can be found during galloping [12]. In fact both have the same result, namely the modification of the external forces, even though the cause is different. Only the former has been taken into account in our model.

To simulate the turbulence it is necessary to model a spatial wind field in a way that the spectrum of energy and the spatial correlation are considered appropriately. To fulfill this need, a wind generator developed by the staff of professor Diana (Politecnico di Milano) is used and the outcoming result is used by our own program to simulate some galloping cases [6] [8].

The wind is generally characterized by the turbulence intensity and the contents of energy for each frequency. Three standard spectrums can be used to describe the longitudinal wind velocity : Harris [2], Davenport [1] and Von Karman [3] spectrums. The turbulence is usually characterized by means of the turbulence intensity :

$$I_u = \frac{\sigma_u}{\bar{U}}$$

where σ_u is the standard deviation of longitudinal wind speed and $\bar{U}$ its average. In this case the vertical component of the turbulence may be important because the angle of attack of the ice deposit is a sensitive factor for galloping. A function based on the theory of isotropic turbulence is used to represent the spectrum of the vertical component.

The figures 1 and 2 show an example of wind recording, made in the experimental site of Villeroux by Laborelec and the corresponding FFT. We can see on the figure 2. that the energy of the turbulence is mainly located in the low frequencies. The turbulence intensity is equal to 24 %.

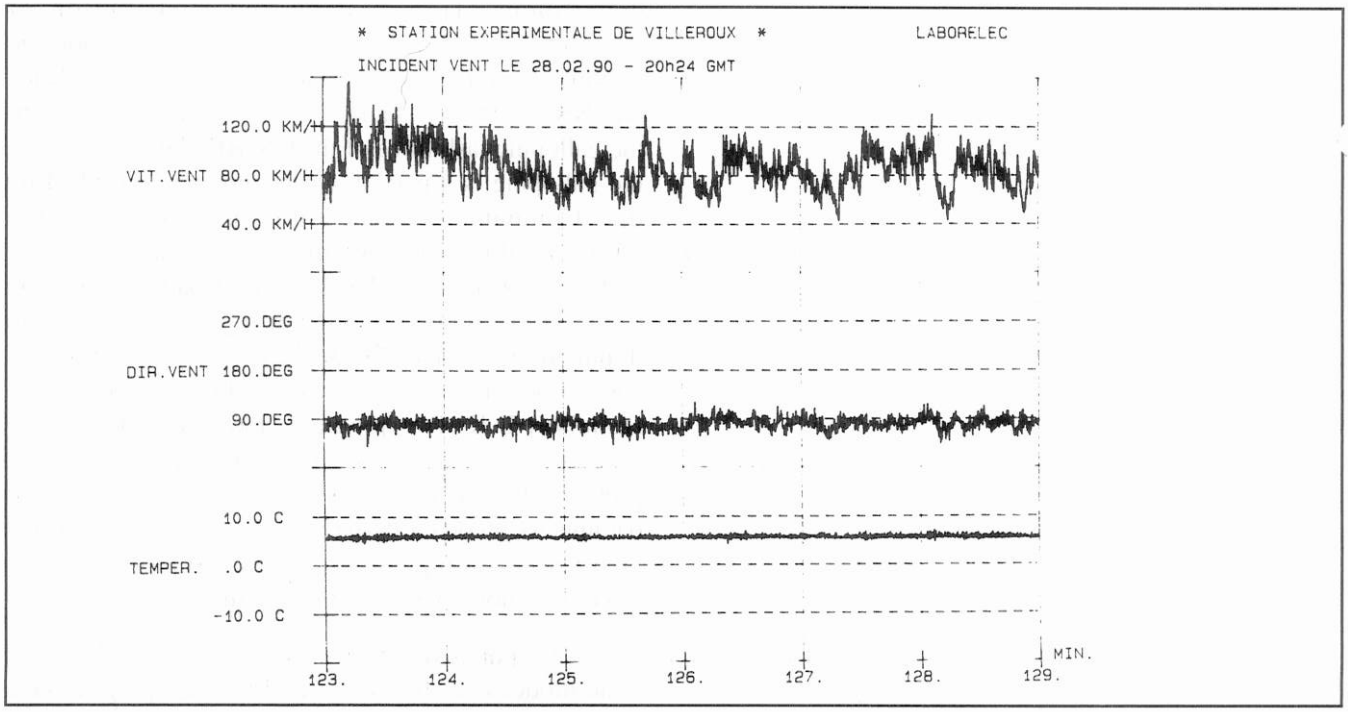

Fig. 1. Recording of the wind, its direction and the temperature in Villeroux (Belgium). Courtesy Mr. Escarmelle, Laborelec.

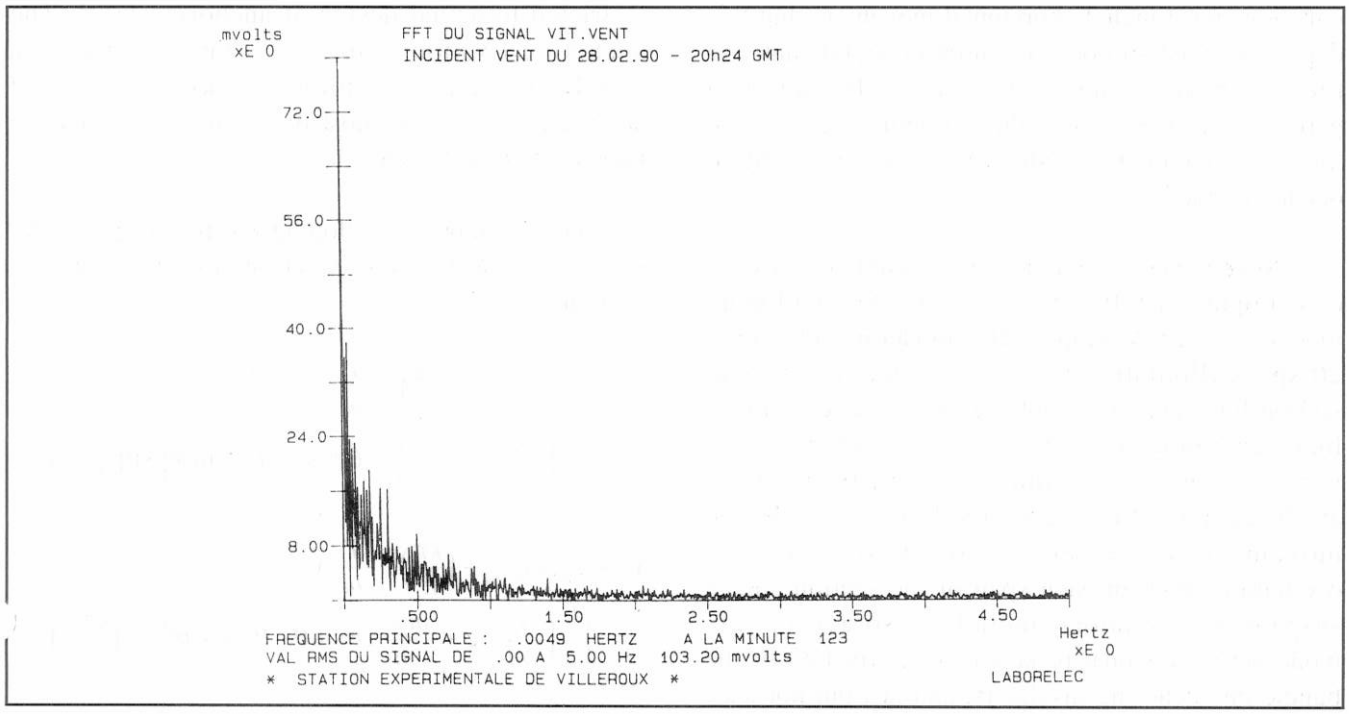

Fig. 2. FFT of the wind recording of the former figure.

Due to the large span length of the overhead transmission lines, the spatial correlation of the wind must be correctly simulated. The coherence function between two point i and j, is interpolated by means of the following relationship :

$$\gamma(f) = e^{-C\frac{f}{\overline{U}}\Delta\zeta}$$

where f is the frequency and $\Delta\zeta$ the distance between the two points. This relation [4] is valid for both the vertical and longitudinal components but the spatial correlation coefficient C can be different for both components.

Description of the analytical galloping model

The galloping phenomenon on bundle conductors is mainly governed by vertical and torsional degree of freedom. In fact, a complete set of

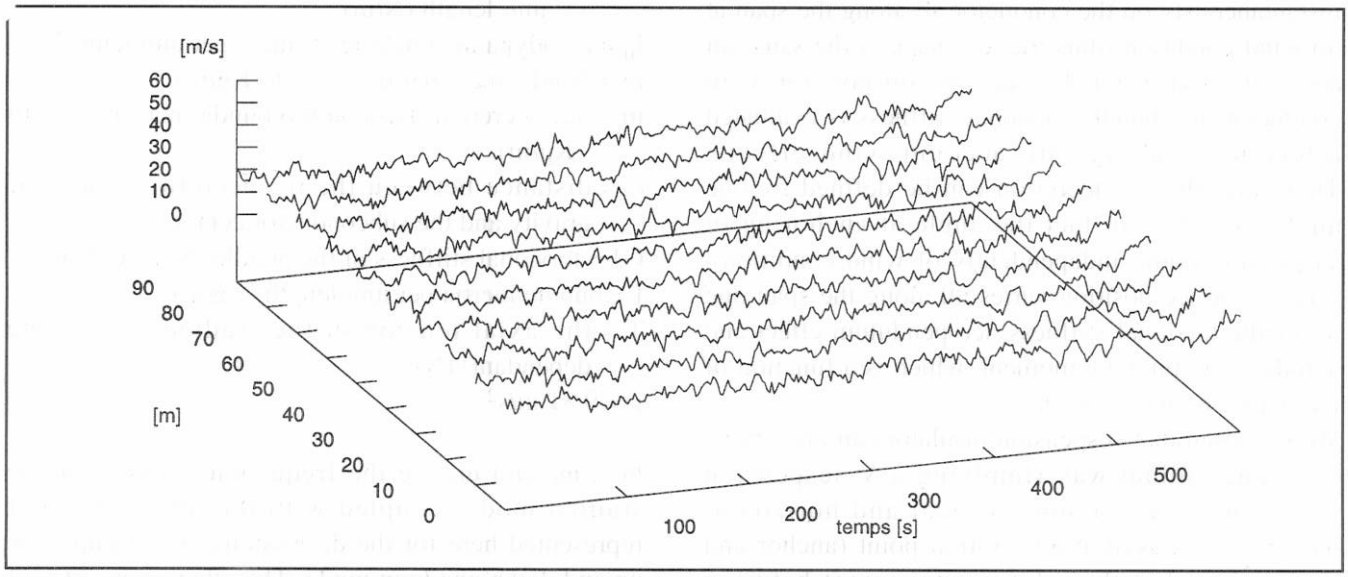

Fig. 3. Example of space-time distribution of the wind.

equations must include horizontal movement, but this degree of freedom doesn't contribute significantly to the instability in most of the case. In fact such participation would force the galloping ellipse to be more horizontal (or 8 shape) which very seldom occurs in practice.

Nevertheless, to include any possible occurrence of galloping, a full 3 degree of freedom galloping model has been developed. This model includes up to 20 spans (limitation is of course due to practical section line data and is not a numerical one), up to 3 loops galloping (more than 3 loops galloping also very seldom occurs and is generally of small amplitude, thus of no interest for design), includes the movement of suspension insulators, tension oscillations both in each span of the section and in suspension insulators, includes also appropriate modeling of torsional behavior of the fixation of the bundle on anchoring insulators, and last but not least the tower stiffness. Anti-galloping devices like pendulums (any position, any orientation) can be simulated either by local effect or distributed one.
In our model horizontal, vertical and torsional damping have been included by equivalent modal viscous damping, inertial and pendulum effects of ice are taken into account. About 15 different kind of ice accretion shape can be used, from very thin (like freezing rain) to very thick (like wet snow), from very light (200 kg/m3) to very heavy (900 kg/m3) density. Quasi-steady aerodynamic curves have been taken from literature and from our own wind tunnel tests.

Ice accretion is supposed to be received instantaneously on the conductor all along the span at no-wind condition (thus the ice shape is the same all along the span) but the equilibrium position with conductor and bundle torsional stiffness is evaluated afterwards, taking into account wind effects. Therefore, the ice accretion can be defined by one angle (which is in fact the angle at anchoring or suspension point, independently of wind condition). Finally, the ice position varies all along the span due to bundle torsional stiffness, ice pendulum effect and aerodynamic pitching moment, which is a function of ice shape and wind speed.
We supposed that suspension insulator can only move in a longitudinal way (implying a V suspension insulator), that torsion, vertical and horizontal movement are zero at all fixation point (anchor and suspension) but the relative movement between subconductors is free at suspension insulator and restricted to actual design at anchoring level. The anchoring fixation in torsion is thus defined by a flexibility matrix which is easily managed automatically for the most of practical cases by the knowledge of yoke plate design.

For one mode of galloping and for one particular span of the section the equations of movement are written [9] :

$$\ddot{y}_k + 2\zeta_v \omega_v \dot{y}_k + \left(\frac{k\pi}{L_s}\right)^2 \frac{T}{m} y_k = \frac{2}{L_s}\int_0^{L_s}\left[\frac{f_v}{m} - g + \frac{m_i d_i}{m}(\ddot{\theta}\cos\theta - \dot{\theta}^2 \sin\theta)\right] \sin\left(\frac{k\pi}{L_s} z\right) dz$$

$$\ddot{x}_k + 2\zeta_h \omega_h \dot{x}_k + \left(\frac{k\pi}{L_s}\right)^2 \frac{T}{m} x_k = \frac{2}{L_s}\int_0^{L_s}\left[\frac{f_h}{m} - g + \frac{m_i d_i}{m}(\ddot{\theta}\sin\theta - \dot{\theta}^2 \cos\theta)\right] \sin\left(\frac{k\pi}{L_s} z\right) dz$$

$$\ddot{\theta}_k + 2\zeta_\theta \omega_\theta \dot{\theta}_k + \left(\frac{k\pi}{L_s}\right)^2 \frac{GJ}{I} \theta_k = \frac{2}{L_s}\int_0^{L_s}\left[\frac{f_\theta}{I} + \frac{m_i d_i}{I}((\ddot{y} + g)\cos\theta - \ddot{x}\sin\theta)\right] \sin\left(\frac{k\pi}{L_s} z\right) dz$$

where,

y, x, θ = global vertical, horizontal and torsional displacement (m)
y_k , x_k , θ_k = k th modal component of the vertical, horizontal and torsional displacement (m)
L_s = span length (m)
ξ_v , ξ_x , ξ_k = vertical, horizontal and torsional damping
f_v , f_x = vertical and horizontal aerodynamic force per unit length (N/m)
f_θ = aerodynamic pitching moment per unit length (N)
m = bundle mass per unit length (Kg/m)
m_i = ice accretion mass on the bundle per unit length (Kg/m)
d_i = distance between the ice accretion center of gravity and the subconductor center (m)
GJ = torsional stiffness of the bundle ($N.m^2$/radian)
I = bundle inertia per unit length (Kg.m)
T = the axial tension in the studied span (time dependant) (N)
g = 9.81 m/s^2

ω_v , ω_h and ω_θ are the frequencies (rad/s) of the studied mode (coupled with the others, but not represented here for the discussion), for example the up and down one loop mode. The other spans interact through the tension T, which is evaluated by an

integration on all the section (all spans between two anchoring towers) length.

To find these equations we have assumed that the global movement is a superposition of three sinus waves :

$$y(z, t) = \sum_{k=1}^{3} y_k(t) \sin(k \pi z/L_s)$$

$$x(z, t) = \sum_{k=1}^{3} x_k(t) \sin(k \pi z/L_s)$$

$$\theta(z, t) = \sum_{k=1}^{3} \theta_k(t) \sin(k \pi z/L_s)$$

but these sinus waves are not the vibration modes, the later ones are in fact a composition of the former ones. Further the sinus modes will be called loops.

Analytical results

Some computations have been performed and here are the results of one case to illustrate what can be obtained. This case is based on the main characteristics of an experimental test line in Japan (Mogami test line, TOKYO EPCO). It is a 360 m long dead-end span with a quad bundle. The spacing is 0.4 m and the cables are ACSR 410 (diameter : 28.5 mm; mass by unit of length : 1.63 Kg/m; tension : 23,500 N). The ice deposit density is 0.6 and its eccentricity is 0.40, it means that the ice thickness is 0.4 times the cable radius (means about 6 mm). The angle of maximum ice accretion is -40 degrees. For the aerodynamic coefficients, the Nigol curves have been selected [11]. The Von Karman spectrum has been used, the longitudinal scale of turbulence of the horizontal component is 90 m and the longitudinal scale of turbulence of the vertical component is 50 m. The spatial correlation coefficient is 7.

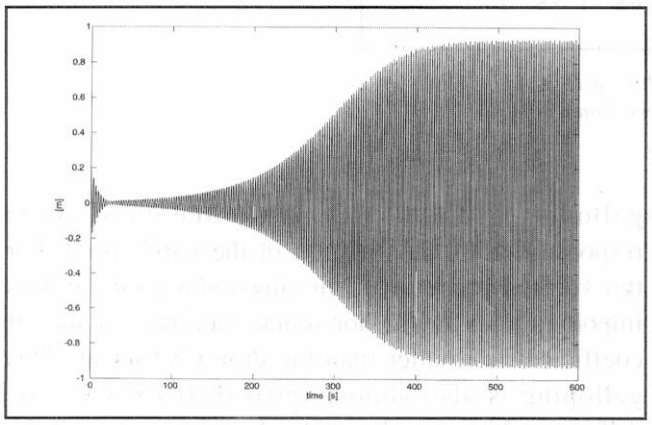

Fig. 4. Vertical displacement at 1/4 span (2-loop component). 12 m/s laminar wind.

This case is a 2-loop vertical oscillation. The figures illustrate the effect of turbulence on the transient period at the beginning of the galloping. Under laminar condition, the instability is excited by means of a small vertical displacement (0.2 m) from the virtual equilibrium position. With a turbulent wind, the transient part is subsequently reduced.

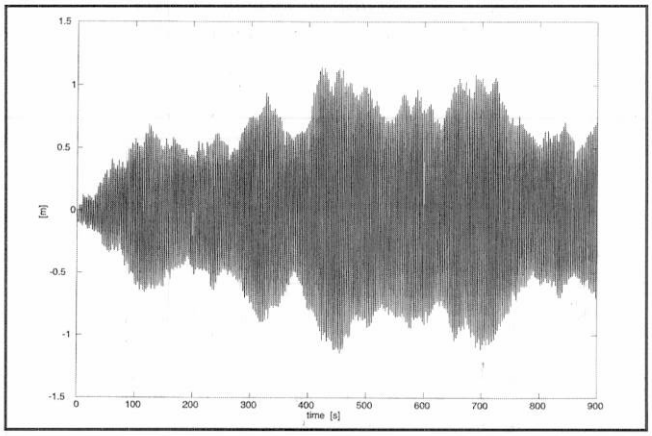

Fig. 5. Vertical displacement at 1/4 span (2-loop component). 12 m/s turbulent wind. $I_u = 0.20$ and $I_w = 0.10$

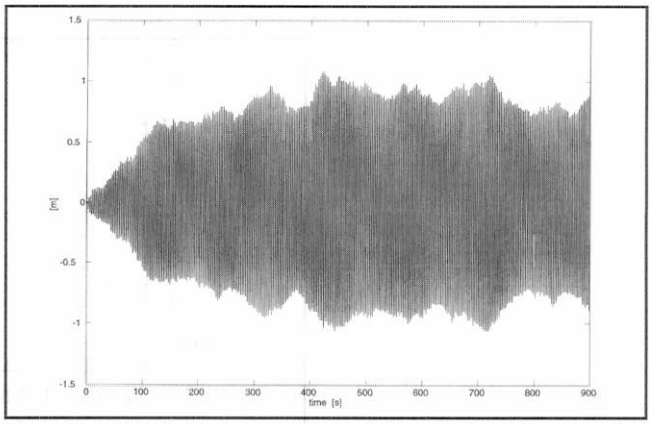

Fig. 6. Vertical displacement at 1/4 span (2-loop component). 12 m/s turbulent wind. $I_u = 0.10$ and $I_w = 0.06$

Next case is similar datas with 18 m/s. The following figures represent the different movements with a laminar wind. The galloping is a very nice periodic oscillation with a frequency of 0.38 Hz. The peak to peak vertical amplitude is 3.2 m and the horizontal one is 0.7. The peak to peak torsional amplitude is about 10 degrees. The galloping ellipse is very thin and almost vertical.

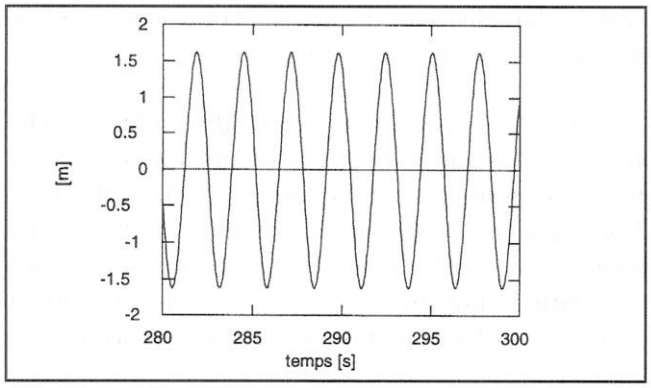

Fig. 7. Vertical displacement at 1/4 span (2-loop component). 18 m/s laminar wind.

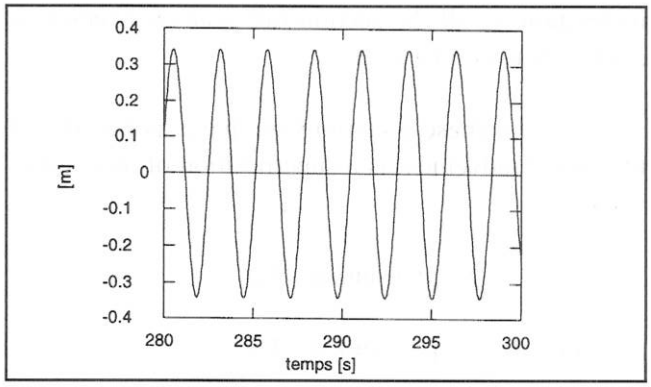

Fig. 8. Horizontal displacement at 1/4 span (2-loop component). 18 m/s laminar wind.

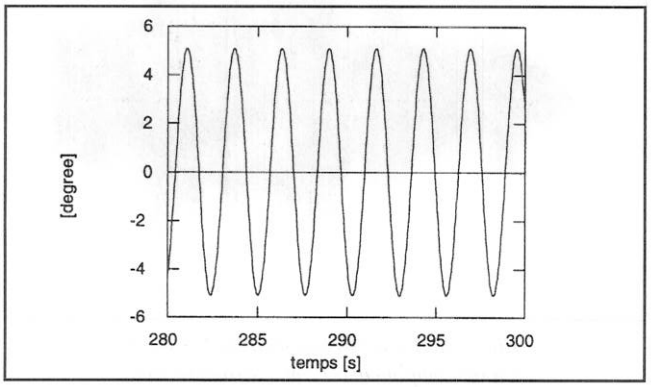

Fig. 9. Torsional movement at 1/4 span (2-loop component). 18 m/s laminar wind.

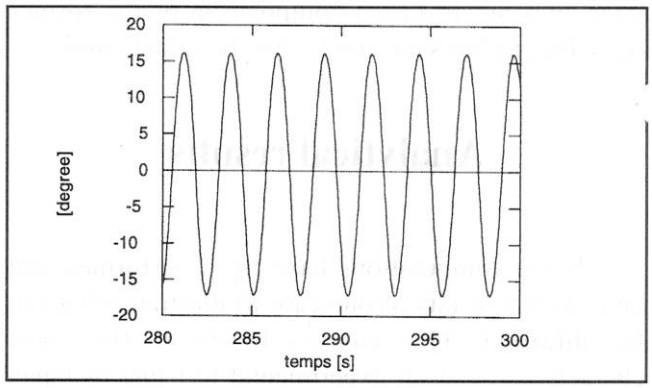

Fig. 10. Angle of attack variation at 1/4 span (2-loop component). 18 m/s laminar wind.

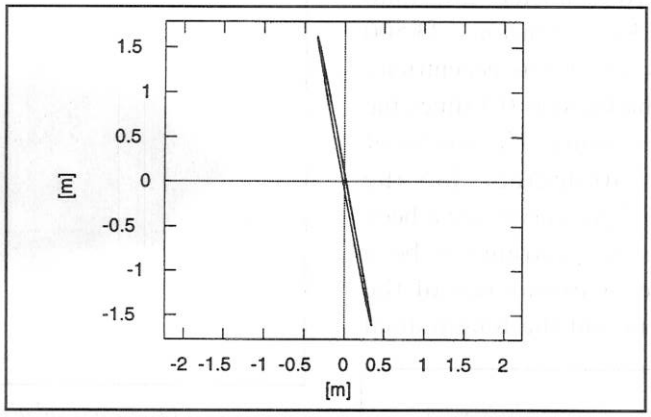

Fig. 11. Galloping ellipse at 1/4 span (2-loop component). 18 m/s laminar wind.

The following figures show the results obtained for the same datas but with a turbulent wind, a horizontal turbulence intensity equal to 20 % and a vertical turbulence intensity equal to 10 %. Except for the horizontal displacement, the results are quite similar to the ones obtained with a laminar wind. The response of the line to the turbulent wind can be divided into two parts. One part is caused by the galloping and the other part is the quasi static response due to the variation of the wind speed. For the vertical movement, the quasi static part is less important than for the horizontal one, because the lift coefficient is smaller than the drag coefficient. This galloping is also almost vertical. It explains the difference between the vertical movement and the horizontal one.

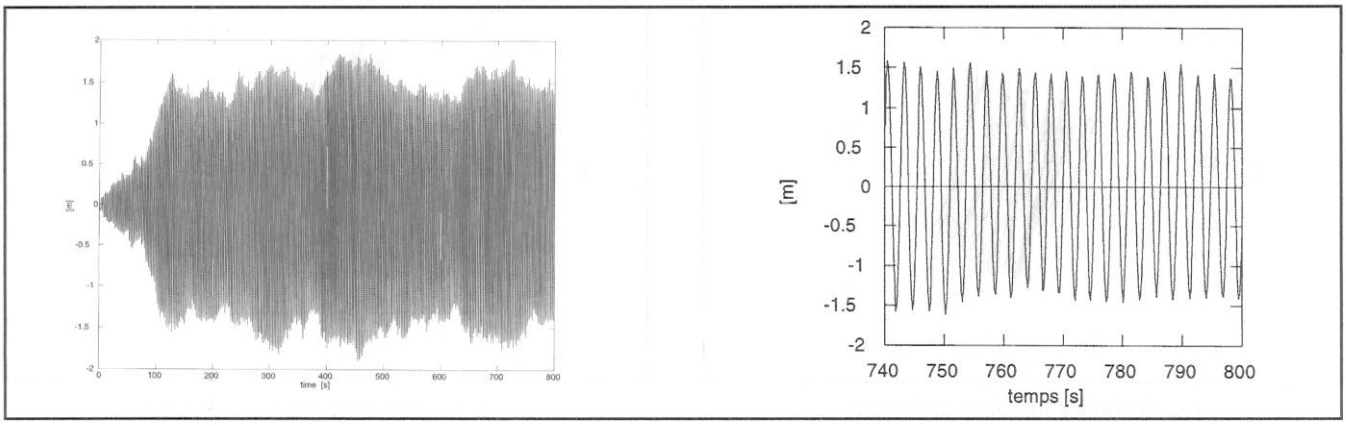

Fig. 12 & 13. Vertical displacement at 1/4 span (2-loop component). 18 m/s turbulent wind. $I_u = 0.20$ and $I_w = 0.10$

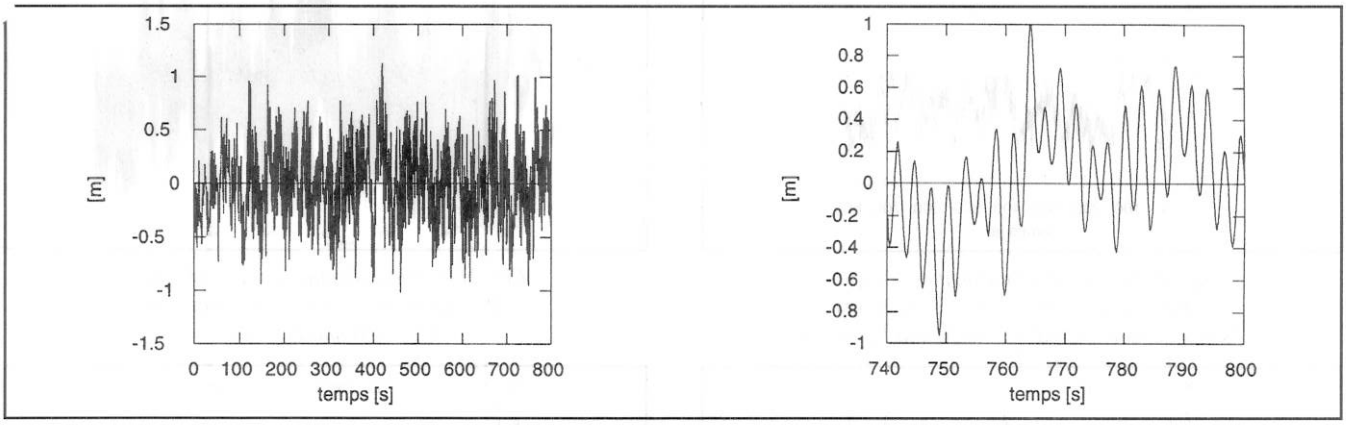

Fig. 14 & 15. Horizontal displacement at 1/4 span (2-loop component). 18 m/s turbulent wind. $I_u = 0.20$ and $I_w = 0.10$

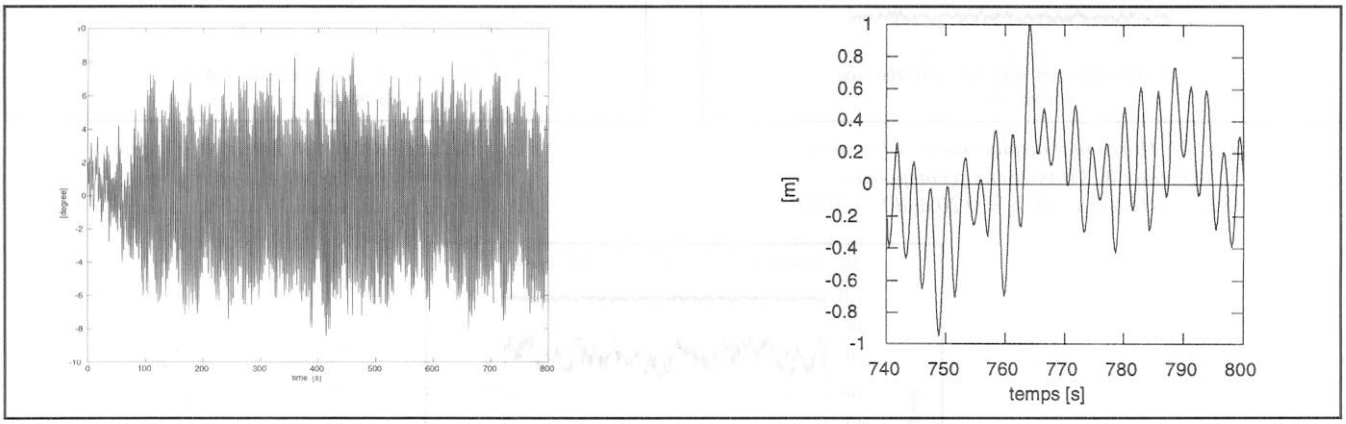

Fig. 16 & 17. Torsional movement at 1/4 span (2-loop component). 18 m/s turbulent wind. $I_u = 0.20$ and $I_w = 0.10$

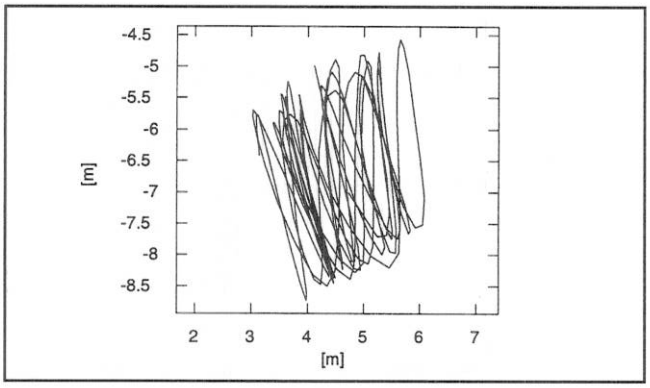

Fig. 18. Galloping ellipse at 1/4 span (all components). 18 m/s turbulent wind. $I_u = 0.20$ and $I_w = 0.10$

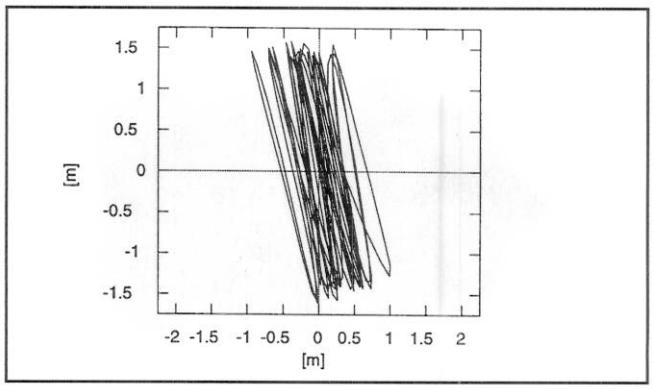

Fig. 19. Galloping ellipse at 1/4 span (2 loop component). 18 m/s turbulent wind. $I_u = 0.20$ and $I_w = 0.10$

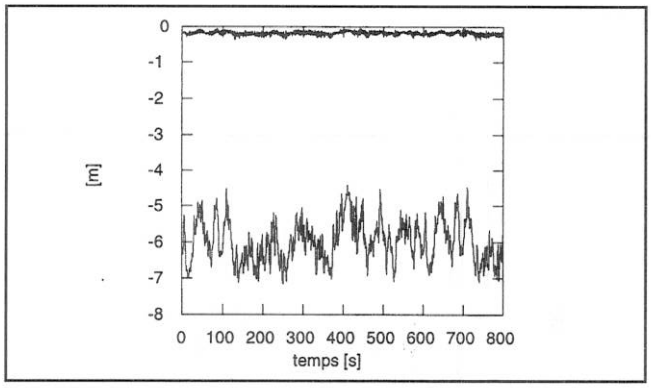

Fig. 20. Vertical displacement at 1/4 span, 1 (below) & 3 (above) loop components. 18 m/s turbulent wind. $I_u = 0.20$ and $I_w = 0.10$

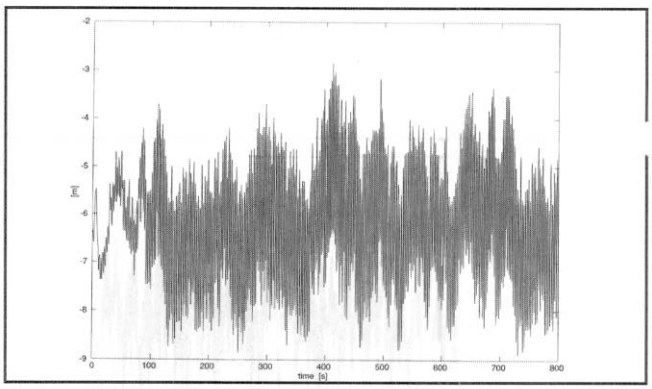

Fig. 21. Vertical displacement at 1/4 span (all components). 18 m/s turbulent wind. $I_u = 0.20$ and $I_w = 0.10$

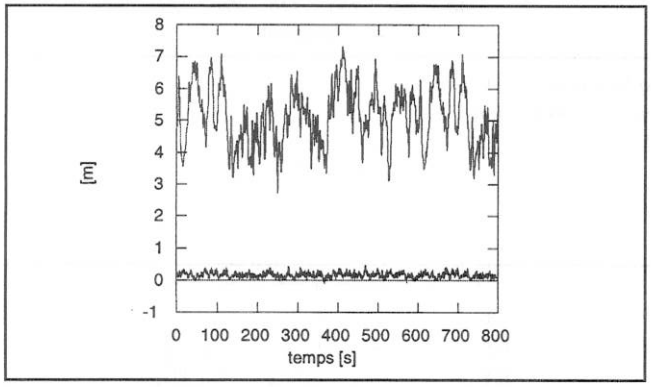

Fig. 22. Horizontal displacement at 1/4 span, 1 (below) & 3 (above) loop components. 18 m/s turbulent wind. $I_u = 0.20$ and $I_w = 0.10$

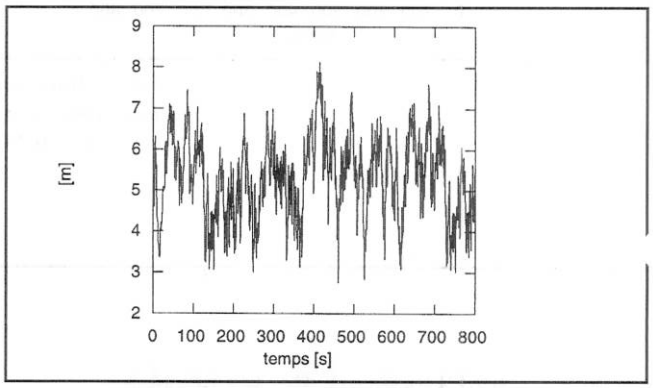

Fig. 23. Horizontal displacement at 1/4 span (all components). 18 m/s turbulent wind. $I_u = 0.20$ and $I_w = 0.10$

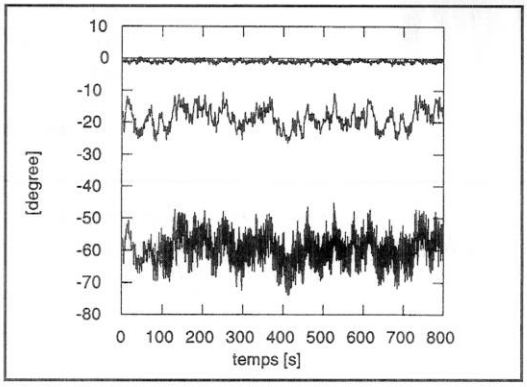

Fig. 24. Torsional movement at 1/4 span, 1 (middle), 3 (above) loop components and complete movement (below).18 m/s turbulent wind. $I_u = 0.20$ and $I_w = 0.10$

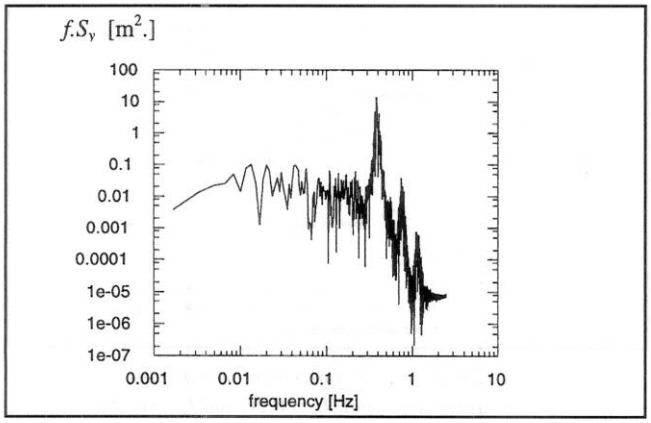

Fig. 25. Power spectrum of the vertical displacement at 1/4 span. 18 m/s turbulent wind. $I_u = 0.20$ and $I_w = 0.10$

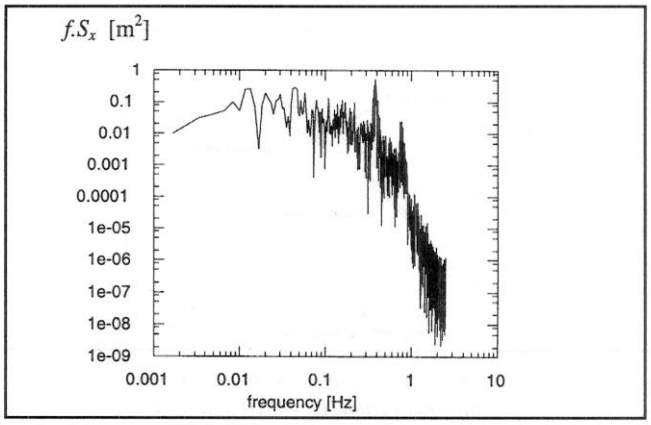

Fig. 26. Power spectrum of the horizontal displacement at 1/4 span. 18 m/s turbulent wind. $I_u = 0.20$ and $I_w = 0.10$

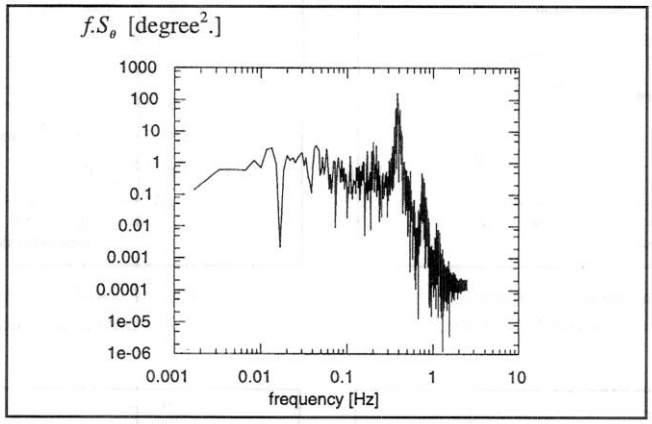

Fig. 27. Power spectrum of the torsional movement at 1/4 span. 18 m/s turbulent wind. $I_u = 0.20$ and $I_w = 0.10$

The peak in the vicinity of 0.4 Hz is the component induced by the galloping of the bundle. The smaller peak in the proximity of 0.75 Hz corresponds to another vibration mode wich includes a 1 loop and a 3 loop component.

For different mean wind speed, we have performed some simulations and we have reported some values on the following figures where we compare these results with the ones for a laminar wind. On the left side are drawn the results with a horizontal turbulence intensity of 10 % and a verticale one of 6 % and on the right side are the results with a horizontal turbulence intensity of 20 % and a verticale one of 10 %. The maximum value of oscillation is always slightly higher than the laminar result except for the horizontal movement where de difference is more important. The mean value is practically always lower than the laminar result but the difference is thin.

Conclusion

The influence of the large scale turbulence in the wind (means the fact that actual wind speed is not constant in time and space) on galloping seems to be very slight. But this instability is so complex and depends on so many factors that it is not possible to draw a conclusion from a single case. There is an increase of the horizontal displacement but it is only due to the turbulence itself and not to an interaction between turbulence and galloping. The maximum vertical displacement (the most important value for the design of the line) increases with the turbulence intensity, but it is not really significant. Surprisingly, the vertical componant of the turbulence has no visible effect on galloping. The greater effect of the turbulence seen in the simulations, is the shortening of the galloping transient (between the threshold and the maximum amplitude). The turbulence effects help

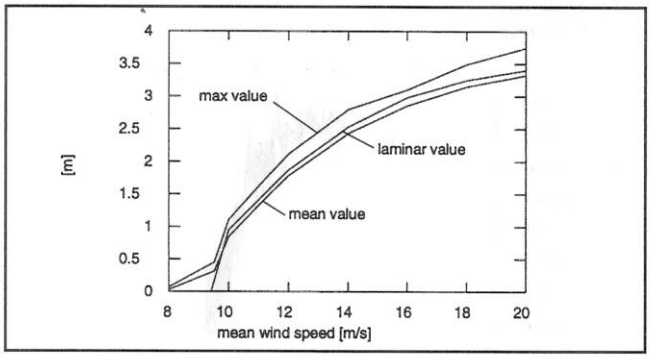

Fig. 28. Vertical displacement at 1/4 span. 18 m/s turbulent wind. $I_u = 0.10$ and $I_w = 0.06$

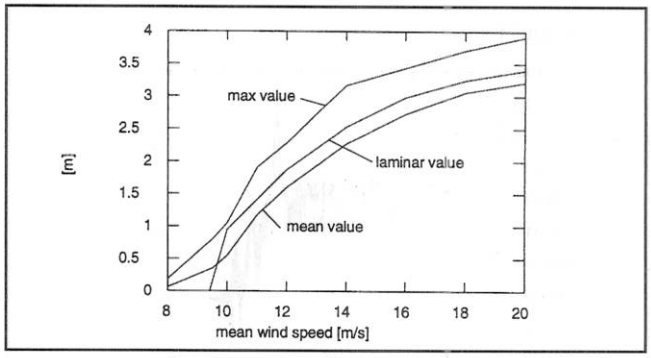

Fig. 29. Vertical displacement at 1/4 span. 18 m/s turbulent wind. $I_u = 0.20$ and $I_w = 0.10$

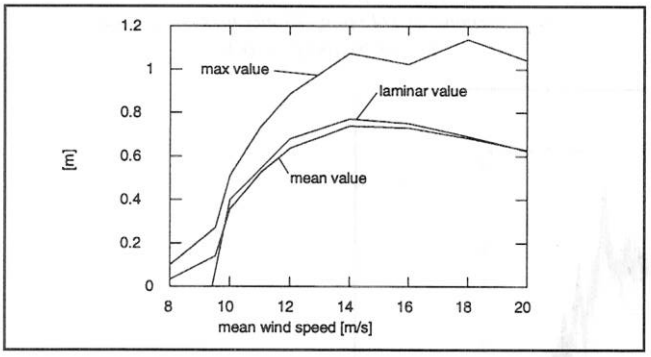

Fig. 30. Horizontal displacement at 1/4 span. 18 m/s turbulent wind. $I_u = 0.10$ and $I_w = 0.06$

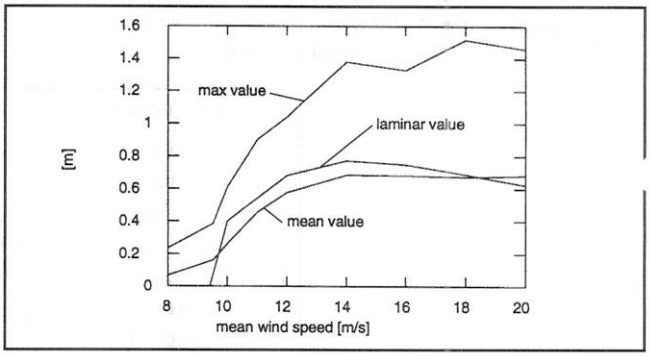

Fig. 31. Horizontal displacement at 1/4 span. 18 m/s turbulent wind. $I_u = 0.20$ and $I_w = 0.10$

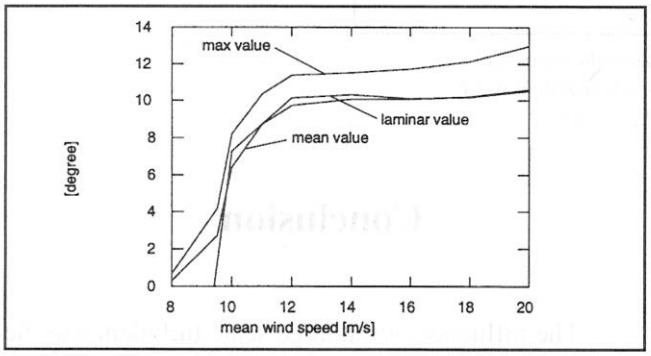

Fig. 32. Torsional movement at 1/4 span. 18 m/s turbulent wind. $I_u = 0.10$ and $I_w = 0.06$

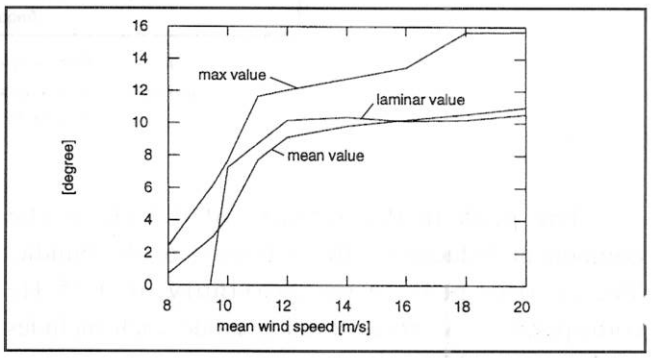

Fig. 33. Torsional movement at 1/4 span. 18 m/s turbulent wind. $I_u = 0.20$ and $I_w = 0.10$

mainly to better fit with actual observations as far as concern transients.

The slight influence of the turbulence on the galloping limit cycle is logical because the modification of the wind speed is not equal on the structure. In fact the characteristic length of the turbulence is quite smaller than the length of the lines generally studied. But another effect of the turbulence is the modification of the aerodynamic characteristics of the iced cable. This factor may be important, but it is not taken into account in this paper because we do not have such kind of data at the present time. Wind tunnel measurements are needed.

Acknowledgement

The authors would like to thank the «Communauté Française de Belgique» for its support and also the staff of Professor Diana for its helpful collaboration.

Appendix : Wind Model

The three spectrums of the longitudinal component of the turbulent wind are :

Harris

$$\frac{f S_u(f)}{\sigma_u^2} = 0.6 \frac{\frac{1800 f}{U_{10}}}{\left[2 + \left(\frac{1800 f}{U_{10}}\right)^2\right]^{5/6}}$$

Davenport

$$\frac{f S_u(f)}{\sigma_u^2} = \frac{2}{3} \frac{\left(\frac{1200 f}{U_{10}}\right)}{\left[1 + \left(\frac{1200 f}{U_{10}}\right)^2\right]^{4/3}}$$

Von Karman

$$\frac{f S_u(f)}{\sigma_u^2} = 4 \frac{\frac{f L_{ux}}{\bar{U}}}{\left[1 + \left(2\,c\,\frac{f L_{ux}}{\bar{U}}\right)^2\right]^{5/6}}$$

où c = 4.2065

where f is the frequency (in Hz), L_{ux} is the longitudinal scale of turbulence, $S_u(f)$ the spectral power density, σ_u^2 represents the RMS of the wind speed in the longitudinal direction, and $\bar{U}$ is the mean wind velocity.

The following function (based on the theory of isotropic turbulence) is used to represent the spectrum of the vertical component :

$$\frac{f S_w(f)}{\sigma_w^2} = 4 \frac{\frac{L_{wx} f}{\bar{U}}}{\left[1 + \left(4\,c\,\frac{L_{wx} f}{\bar{U}}\right)^2\right]^{11/6}} \left[1 = \frac{128}{3}\left(c\,\frac{L_{wx} f}{\bar{U}}\right)^2\right]$$

where L_{wx} is the longitudinal scale of turbulence of the vertical component, $S_w(f)$ the spectral power density of the vertical component and σ_w^2 is the variance of the vertical component.

References

[1] A. G. Davenport, *The spectrum of Horizontal Gustiness Near the Ground in High Winds*, J. Royal Meteorol. Soc. , 87, 1961, pp. 194-211.

[2] R. Harris, *The nature of the Wind*, CIRIA Seinar on the Modern Design of Wind-sensitive Structures, London, 1970.

[3] H. PA. H. Irwin, *Wind Tunnel and Analytical Investigation of the Response of Lion's Gate Bridge to a Turbulent Wind*, LTR-LA-210, National Research Council Canada, June 1977.

[4] A. G. Davenport, *The Dependence of Wind Load upon Meteorological Parameters*, in Proceedings of The international Research Seminar on Wind Effects on Buildings and Structures, University of Toronto Press, Toronto, 1968, pp. 19-82.

[5] E. Simiu, R. H. Scanlan, *Wind Effects on Structure*, John Wiley and Sons, New York, second edition, 1986.

[6] M. Bocciolone, F. Cheli, A. Curami, A. Zasso, *Wind Measurements on the Humber Bridge and Numerical Simulations*, Journal of Wind Engineering and Industrial Aerodynamics, Elsevier, 41-44, 1992, pp. 1393-1404.

[7] P. Duchène, Marullaz, *Full Scale Measurement of Atmospheric Turbulence in a Suburban Area*, Centre Scientifique de Tecnique du Bâtiment, Nantes, 1965.

[8] G. Diana, F. Cheli, P. Nicolini, F. Tavano, *Oscillations of Bundle Conductors in Overhead Lines Due to Turbulent Wind*, 90 WM 112-3 PWRD, IEEE, Italy,1990.

[9] J.L. Lilien, O. Chabart, *High Voltage Overhead Lines Three Mechanisms to Avoid Bundle Galloping*, International Symposium on Cable Dynamics, Liège (Belgium), October 1995, pp 381-390.

[10] A. Preumont, *Vibrations Aléatoires et Analyse Spectrale*, Presses Polytechniques Romandes, Lausanne, 1990.

[11] O. Nigol, G. J. Clarke, D. G. Havard, IEEE Trans, PAS, vol. 96, n. 5, sept. 1977, pp. 1666-1674.

[12] A. G. Davenport, *The Dynamics of Cables in Wind*, International Symposium on Cable Dynamics, Liège (Belgium), October 1995.

ÉTUDE D'ALGORITHMES DE RÉSOLUTION DE CONTRAINTES NUMÉRIQUES BASÉS SUR LES AUTOMATES

L. BRONNE
Lauréat du Prix Melchior Salier
Orientation Informatique
Année académique 1995-1996

1. Introduction

Le principal problème dans le cadre de la vérification automatique de programmes est l'explosion de la taille de l'espace des états. Diverses méthodes tendent à modérer cette taille. À côté des techniques qui consistent à limiter la recherche aux seuls états utiles pour la propriété à vérifier (par exemple les techniques d'ordres partiels [WG93, God94]), ont été développées des techniques permettant de représenter de manière symbolique des ensembles d'états.

Dans de nombreux domaines (par exemple l'analyse de systèmes «temps réel» [AH90,ACD90]), les états sont caractérisés par des valeurs entières ou réelles. Des techniques de représentation d'ensembles d'entiers ou de réels ont donc été introduites. Ces ensembles sont habituellement représentés par des formules composées de variables, de constantes, d'opérateurs arithmétiques, de relations d'ordre et d'opérateurs logiques. Nous verrons dans la section 2 que certaines de ces formules peuvent être représentées au moyen d'automates.

Le but de ce travail est l'utilisation d'automates représentant des ensembles d'entiers pour en tirer des méthodes algorithmiques de résolution de problèmes de contraintes. La section 2 présente le type d'automates concurrents que nous utiliserons. Déterminer la consistance d'une formule reviendra à déterminer si l'automate correspondant à la formule accepte un langage non vide. Ce problème est PSPACE-complet.

La section 3 donne une application où l'exploration de l'espace des états peut être réalisée de manière polynomiale : les systèmes d'inégalités arithmétiques. Après avoir montré que la recherche dans l'espace des états peut être réalisée sans retour